Geophys. J. R. astr. Soc. (1984) **76**, 89–111

The magnitude, symmetry and origin of upper mantle anisotropy based on fabric analyses of ultramafic tectonites

Nikolas I. Christensen* *Department of Geophysics and Graduate Program in Geophysics, University of Washington, Seattle, Washington 98125, USA*

Received 1983 February 21

Summary. Seismic anisotropy within the upper mantle originates from the preferred orientation of highly anisotropic single crystals. The symmetry and magnitude of anisotropy depend upon: (1) the volume percentages of the minerals constituting the upper mantle, (2) the degree and symmetry of preferred orientation of each mineral and (3) the alignment of the minerals' crystallographic axes relative to one another. The nature of upper mantle anisotropy can be examined by studying mineral orientations within ultramafic rocks which were once part of the mantle. Petrofabric data for olivine and pyroxene have been used to obtain velocity anisotropy patterns over large regions of ultramafic rocks from the Samail ophiolite, Oman, the Troodos ophiolite, Cyprus, the Bay of Islands ophiolife, Newfoundland, the Twin Sisters ultramafic, Washington, USA, the Dun Mountain ophiolite, New Zealand, the Red Hills ophiolite, New Zealand and the Red Mountain ophiolite, New Zealand. The compressional wave anisotropy calculated for these massifs ranges from 3 to 8 per cent, in excellent agreement with observed seismic anisotropy in the upper continental and oceanic mantle. The symmetry varies from orthorhombic to axial, with the axial symmetry axis corresponding to the olivine *a*-axes maxima and subparallel to spreading directions in oceanic upper mantle. Pyroxene *a*-, *b*- and *c*-axes maxima generally parallel olivine *b*-, *c*- and *a*-axes, respectively, and anisotropy decreases with increasing pyroxene content. Shear-wave splitting is predicted for all propagation directions within the upper mantle. Symmetry is also orthorhombic or axial, with the minimum difference in velocity between the two shear-waves parallel to the maximum compressional wave velocity.

1 Introduction

In 1964 Harry Hess published evidence which suggested that the upper mantle was anisotropic to compressional-wave propagation. Hess' observation was based on P_n velocities obtained by Raitt (1963) and Shor & Pollard (1964) in the Mendocino and Maui areas of the north-east Pacific. Plots of velocities versus azimuth in these regions showed that upper mantle compressional-wave velocities were fast for propagation directions approximately

*Present address: Department of Geosciences, Purdue University, West Lafayette, Indiana 47907, USA.

Figure 1. Observed upper mantle anisotropy. Arrows indicate directions of maximum velocity (see text for references).

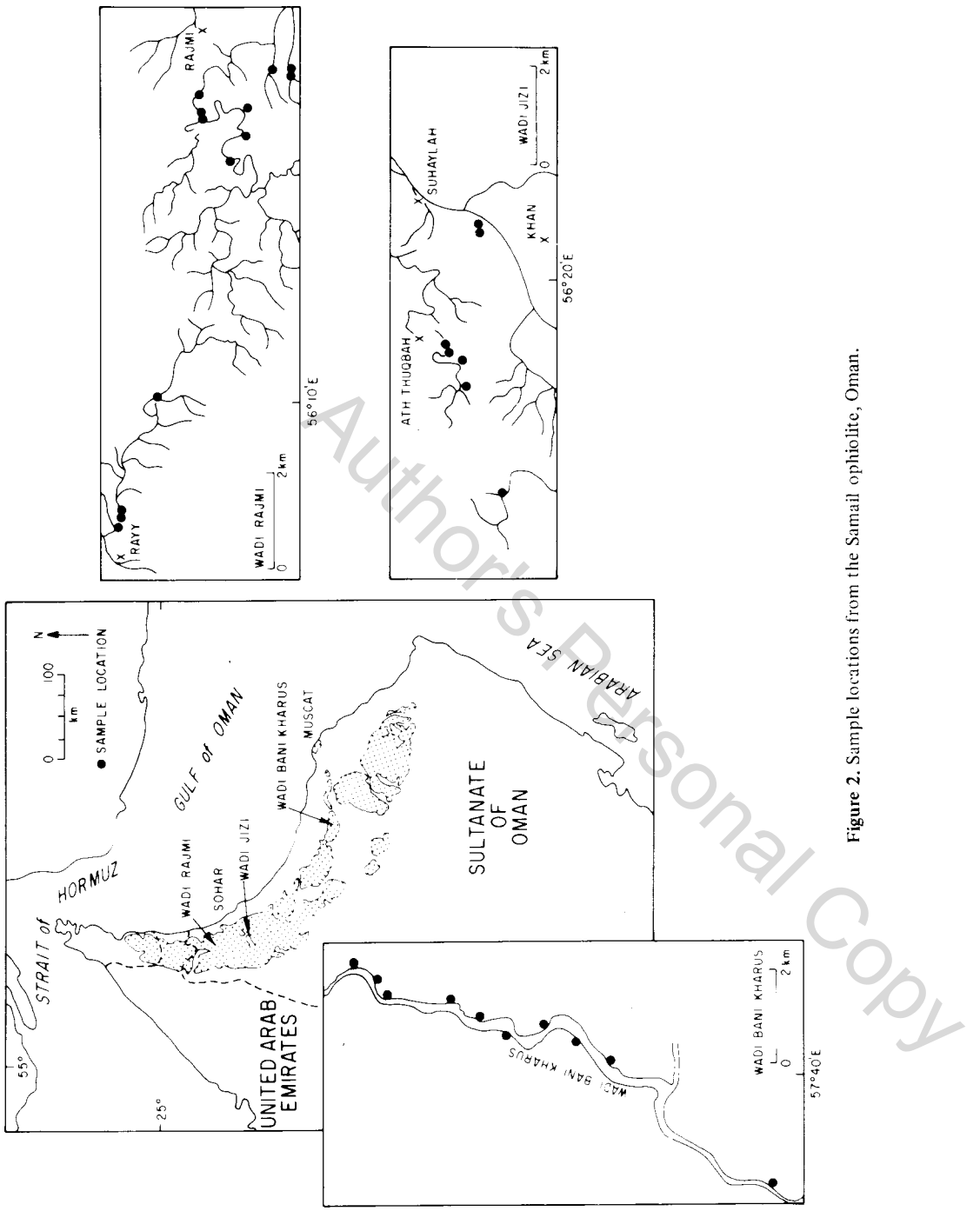

Figure 2. Sample locations from the Samail ophiolite, Oman.

parallel to fracture zones. More recent detailed refraction studies have clearly demonstrated that seismic anisotropy is a common phenomenon in the oceanic upper mantle (Raitt *et al.* 1969; Morris, Raitt & Shor 1969; Raitt *et al.* 1971; Keen & Barrett 1971; Shor *et al.* 1973; Snydsman, Lewis & McClain 1975; Malecek & Clowes 1978) and continental upper mantle (Bamford 1977; Bamford, Jentsch & Prodehl 1979; Vetter & Minster 1981; Fuchs 1984). Fig. 1 shows the directions of maximum velocities and the magnitudes of the anisotropies. There is evidence that mantle anisotropy may extend to considerable depth (Leven, Jackson & Ringwood 1981; Dziewonski & Anderson 1981).

Hess (1964) proposed that mantle anisotropy originated from preferred olivine orientation. It was known from measurements in Dunbar laboratory at Harvard University

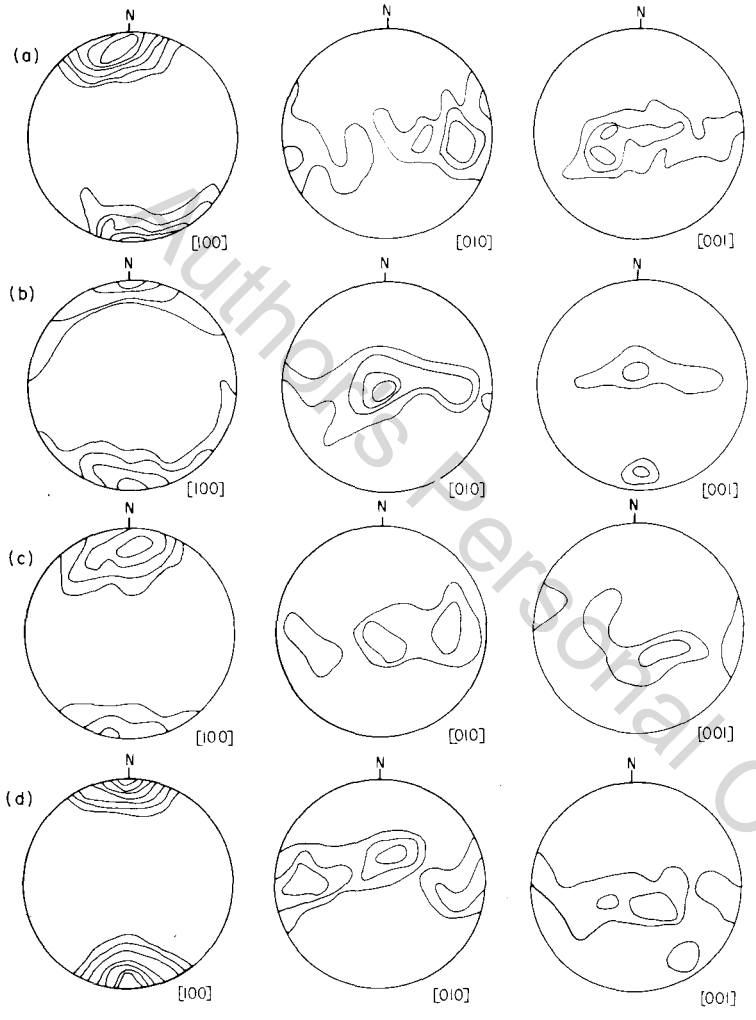

Figure 3. Composite olivine equal-area lower-hemisphere projections of {100}, {010} and {001} axes from: (a) Wadi Rajmi, Oman; (b) Wadi Jizi, Oman; (c) Wadi Bani Kharus, Oman; (d) Troodos, Cyprus; (e) Table Mountain, Newfoundland; (f) North Arm Mountain, Newfoundland; (g) Blow Me Down Mountain, Newfoundland; (h) Lewis Hills, Newfoundland; (i) Twin Sisters, USA; (j) Red Mountain, New Zealand; (k) Dun Mountain, New Zealand; and (l) Red Hills, New Zealand. The projections are contoured in 2σ intervals with the lowest contour = 4σ. A density of 3σ indicates a uniform distribution of points and is equal to the number of points divided by the counting area (Kamb 1959).

(Verma 1960; Birch 1960, 1961) that single crystal olivine is highly anisotropic, with compressional-wave velocities at atmospheric pressure of 9.87, 7.73 and 8.65 km s^{-1} in the *a*, *b* and *c* crystallographic directions, respectively, and that many ultramafic rocks are highly anisotropic to compressional-wave propagation, presumably due to preferred olivine orientation. Hess (1964) postulated that olivine [010] crystallographic planes are aligned subparallel to major oceanic fracture zones, which explains the observed low velocities normal to fracture zones. Later, Francis (1969), citing the deformation experiments of Raleigh (1968) on olivine, proposed that the anisotropy originated from plastic flow in which the olivine crystallographic *a*-axis aligned parallel to flow directions in the upper mantle.

Detailed studies of olivine fabrics in ultramafic rocks combined with velocity measurements at elevated pressures (Christensen 1966, 1971a; Christensen & Ramananantoandro 1971; Babuška 1972; Carter, Baker & George 1972; Peselnick & Nicolas 1978) have subsequently confirmed that seismic anisotropy in ultramafic rocks is related to preferred mineral orientation. Laboratory studies have also shown that shear-wave anisotropy is an important property of ultramafic rocks (Christensen 1966, 1971b; Christensen &

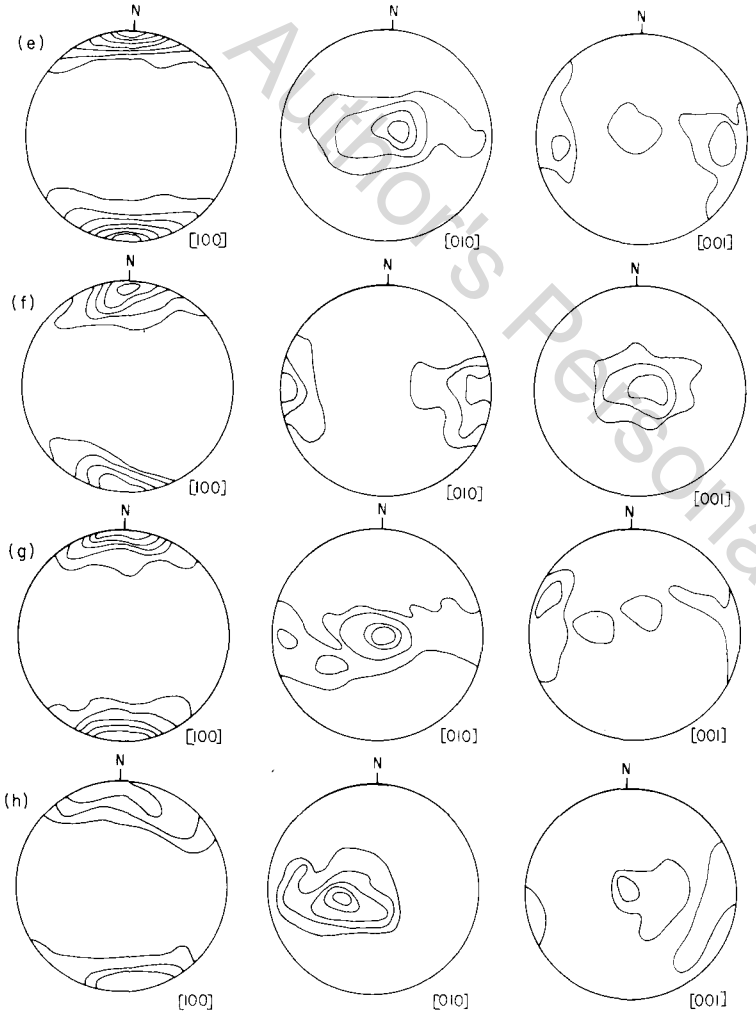

Figure 3 – *continued*

Ramananantoandro 1971i) and variations of shear-wave velocity with azimuth as well as shear-wave splitting are likely to be encountered in upper mantle seismic studies.

Since seismic refraction profiles designed to study upper mantle velocity structure are several tens of kilometres in length and cover large areas, caution must be exercised in correlating velocity information from a single rock sample with observed mantle anisotropy. Clearly it is more desirable to compare mantle seismic anisotropy data with laboratory measurements obtained from multiple samples collected over large areas. Some ultramafic massifs, which presumably originated within the Earth's mantle, have regional olivine fabric patterns which produce overall anisotropy comparable with mantle seismic anisotropy (Christensen 1971a; Peselnick & Nicolas 1978; Christensen & Salisbury 1979). Within these massifs the degree of preferred mineral orientation and the symmetries often vary significantly from one locality to another; however, the directions of maximum concentrations of some crystallographic axes are often surprisingly consistent.

In this paper detailed seismic anisotropies, based on petrofabric analyses of minerals from multiple samples, are presented for several ultramafic massifs believed to have upper mantle origins. It is shown that the magnitudes and symmetries of compressional- and shear-wave

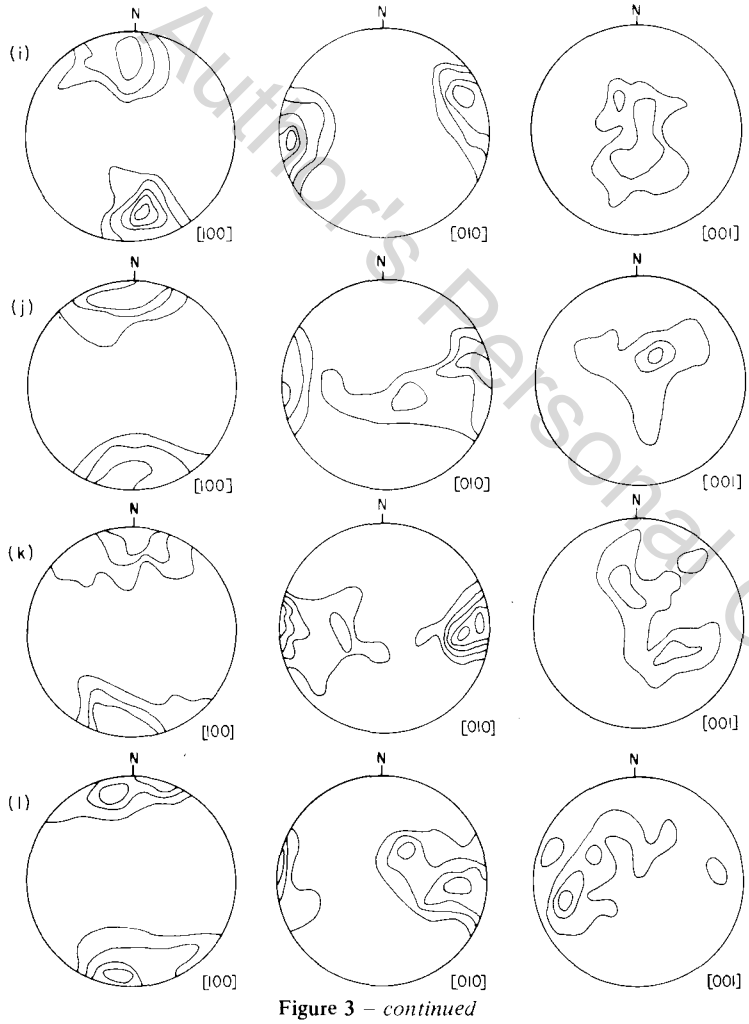

Figure 3 – *continued*

anisotropies of ultramafic massifs from Oman, Cyprus, Newfoundland, the United States and New Zealand possess remarkable similarities with one another. Furthermore, when the influences of accessory mineralogy and temperature are taken into account, there is excellent agreement between observed upper mantle seismic anisotropy and the anisotropy present in the ultramafic massifs.

2 Anisotropy calculations

The procedure used in this paper to obtain overall anisotropy in the ultramafics is similar to that outlined by Christensen & Salisbury (1979). Oriented field samples of dunite and peridotite have been collected throughout each ultramafic massif. The density and distribution of samples depended on a variety of factors, including accessibility, structural information available from previously published maps and field observations obtained during the collecting. For all massifs the sampling objective was to obtain as representative a suite of samples as possible, which would give valid overall seismic properties of the whole or portion of the massif under investigation.

Horizontal rock slices were cut from the field-oriented specimens. Oriented thin sections were made from the slices, which were photographed and mounted between hemispheres on a 5-axis universal stage equipped with a proper upper hemisphere and slide for fabric analyses. Usually 100 olivine grains were selected for orientation from each specimen. Each grain was located on the photograph and rotations of the universal stage axes and positions of the olivine axes after orientation were recorded for each grain. The orientations of the olivine axes were plotted and contoured by computer for each specimen using the contouring method described by Kamb (1959). In addition, composite fabric diagrams for each ultramafic massif or portion of massif under investigation have been contoured using the total olivine orientation data from each massif.

Rather than using a 1 per cent counting circle as is commonly done with the Mellis technique, the Kamb method of contouring employs a variable size counting circle of large enough size so that it will repeatedly obtain densities close to the expected number for a randomly populated net. The counting circle is calculated to be large enough so that 99 per cent of the time (within ± 3 standard deviation), the circle will enclose the expected number for a randomly distributed population. The Kamb technique eliminates spurious points on a typical contoured net and separates the net into regions that are significantly and not significantly overpopulated.

The composite fabric diagrams have been used to calculate the overall anisotropy of each ultramafic body using the elastic constants of olivine and their pressure derivatives. Calculations of this type were first performed by Kumazawa (1964) for hypothetical olivine aggregates having relatively simple fabric symmetry. More recent detailed calculations of anisotropy from olivine petrofabric data have been shown to agree well with laboratory measured velocities (Klima & Babuška 1968; Crosson & Lin 1971; Baker & Carter 1972; Carter *et al.* 1972; Peselnick & Nicolas 1978).

The velocity anisotropy presented for each massif in this paper has been obtained using the technique described by Crosson & Lin (1971), the elastic constants of olivine and their pressure derivatives at ambient temperature (Kumazawa & Anderson 1969), the total olivine orientation data for each massif, and the density of olivine. The solution of the Cristoffel equation for any given wave normal gives three velocities which correspond, in general, to one quasi-compressional and two quasi shear-waves (e.g. Musgrave 1970). The two quasi shear-waves are orthogonally polarized and travel at different velocities for most directions of propagation. Contour diagrams of the compressional-wave velocities, as well as the difference in velocity between the two quasi shear-waves, ΔV_S, which is a measure of shear-wave splitting (Crampin 1981), have been constructed for each ultramafic massif.

In the following section it is shown that the most distinctive feature of each composite olivine fabric is a strong crystallographic *a*-axis maximum. For comparison purposes the olivine field oriented fabric diagrams have been rotated so the olivine *a*-axis maxima are horizontal or nearly horizontal and north–south. The velocity anisotropy diagrams have also been rotated to correspond to fabric orientations.

3 Olivine fabrics and mantle anisotropies

3.1 SAMAIL OPHIOLITE – OMAN

The Samail ophiolite, a section of Tethyan ocean crust and upper mantle and one of the largest and best exposed ophiolites in the world, has recently been the subject of several detailed geological and geophysical investigations (e.g. Coleman 1981; Coleman & Hopson 1981; Smewing 1981). The massif is believed to have formed at a spreading centre of Middle

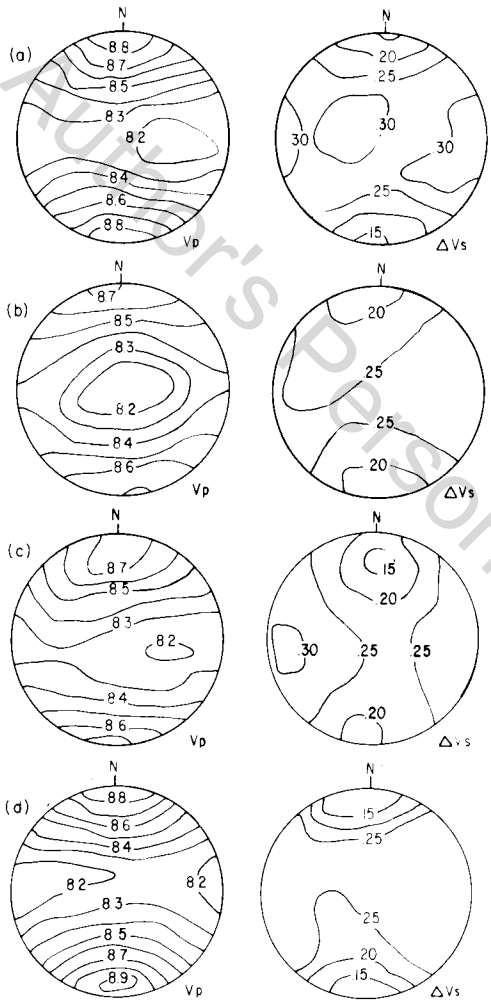

Figure 4. Anisotropy of compressional wave velocity and shear-wave splitting (ΔV_S) in km s^{-1} at 2 kb confining pressure shown as lower hemisphere projections. Locations are given in caption for Fig. 3.

Cretaceous age and subsequently obducted on to the Arabian continental margin during the Late Cretaceous.

Located in the Sultanate of Oman south-west of the Gulf of Oman, the ophiolite forms a belt 475 km long and up to 80 km wide (Fig. 2). A complete section up to 18 km in thickness of marine sediments, pillow basalts, sheeted dykes, gabbro and peridotite is present in the central and northern portions of the ophiolite. Mapping on the scale of 1:500,000 by Glennie *et al.* (1974) has shown that faulting has cut the ophiolite into several blocks generally ranging from a few kilometres to 25 km in width. The mafic crustal section is 6–7 km in thickness (Hopson *et al.* 1981; Christensen & Smewing 1981) and complete sections of ultramafic mantle up to 10 km in thickness are well exposed within the fault blocks.

Samples collected for the present study were obtained along three widely separated traverses, designated Wadi Rajmi, Wadi Jizi and Wadi Bani Kharus (Fig. 2). Composite olivine fabric diagrams are shown in Fig. 3 and the velocities and seismic anisotropies for these sections of the ophiolite are given in Fig. 4.

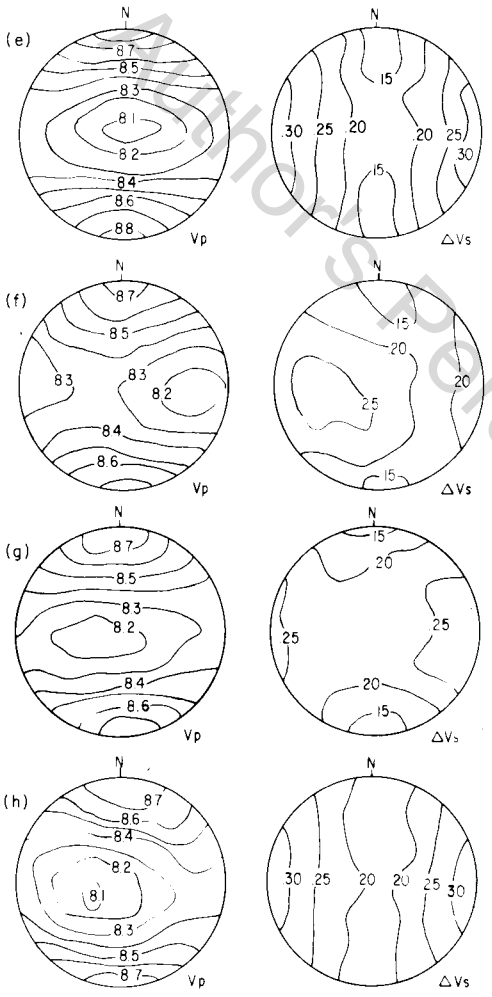

Figure 4 – *continued*

3.2 TROODOS OPHIOLITE – CYPRUS

The Troodos ophiolite of Cyprus has been the subject of numerous geological studies and like the Samail ophiolite consists of a complete stratigraphic sequence ranging downward from pillow basalts through sheeted dykes and gabbros to ultramafic tectonites (e.g. Wilson 1959; Gass & Smewing 1973; Moores & Vine 1971; Greenbaum 1972). It is Upper Cretaceous in age and is exposed in an area roughly 90 x 30 km. The upper mantle rocks crop out in the central portion of the massif, whereas the pillow lavas occur along the periphery (Fig. 5).

The ultramafic rocks consist of cumulate and tectonized dunites and harzburgites (Greenbaum 1972; George 1978). Structure within the ultramafic portion of the ophiolite is complicated by the presence of a serpentinite diapir beneath the summit of Mount Olympus and numerous faults. Locations of samples selected for this study (Fig. 5) show a fairly consistent olivine fabric (Fig. 3). However, it should be noted that a relatively small number of samples have been studied and previous petrofabric analyses by George (1978) suggest a considerably more complicated olivine orientation pattern within the whole

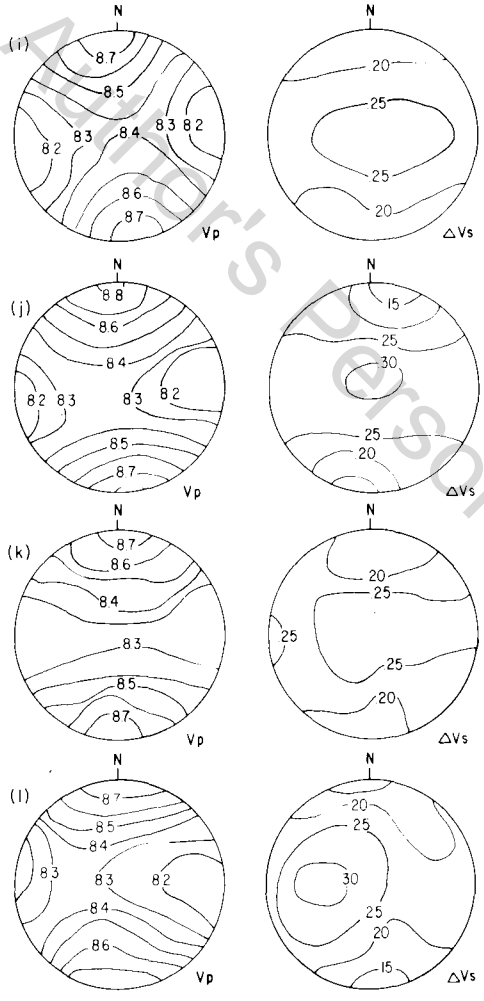

Figure 4 – *continued*

ultramafic portion of the ophiolite. Calculated anisotropies from the olivine composite of Fig. 3 are shown in Fig. 4.

3.3 BAY OF ISLANDS OPHIOLITE – NEWFOUNDLAND

Like the Troodos and Samail ophiolites, the Bay of Islands ophiolite complex, located in western Newfoundland, consists of volcanics, sheeted dykes, gabbros and peridotites. The Bay of Islands ophiolite is believed to have originated as a segment of the 'proto-Atlantic' oceanic crust and upper mantle (Church 1972). Obduction took place during Ordovician as part of the closing of the proto-Atlantic Ocean (Williams & Stevens 1974).

The Bay of Islands complex consists of four separate massifs which extend in a NE–SW trending belt approximately 100 km long and 25 km in width (Williams 1973). In the northernmost massif, Table Mountain, the upper crustal section has been eroded leaving only the lower gabbro and ultramafic sections, whereas the crustal sections in North Arm Mountain and Blow Me Down Mountain are complete or nearly complete (Fig. 6). The southernmost massif, Lewis Hills, contains abundant gabbro and ultramafics along with some volcanics and dyke rocks (Smith 1958; Williams & Malpas 1972; Karson 1982). The ultramafic rocks consist primarily of harzburgite with subordinate dunite and are strongly tectonized (Smith 1958; Christensen & Salisbury 1979; Girardeau & Nicolas 1981). A crude layering originating from a variation in the olivine-orthopyroxene ratio is sometimes observed and a well-defined foliation produced by mineral alignment and flattening is common.

Olivine fabrics and calculated anisotropies reported by Christensen & Salisbury (1979) for Table Mountain and North Arm Mountain are shown in Figs 3 and 4. The locations of samples used for the composite calculations are given in Fig. 6. New data for olivine fabrics and seismic anisotropy in the ultramafic sections of Lewis Hills and Blow Me Down Mountain are also presented in Figs 3 and 4.

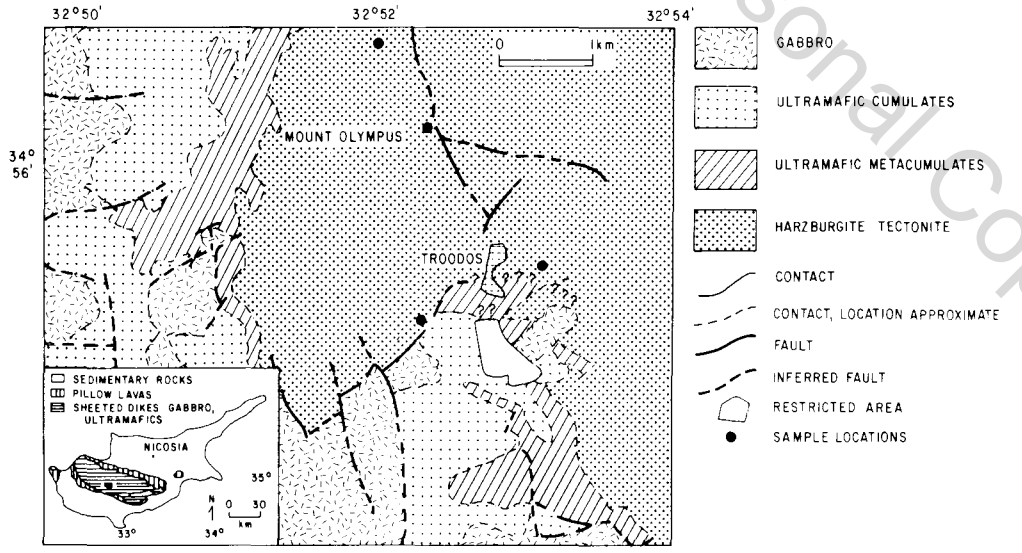

Figure 5. Sample locations from the Troodos ophiolite, Cyprus.

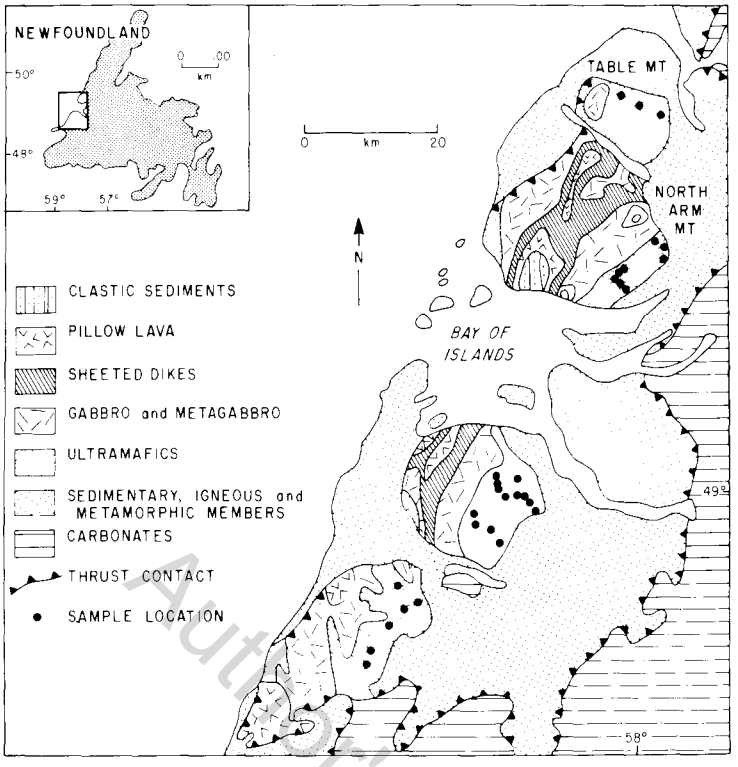

Figure 6. Sample locations from the Bay of Islands ophiolite, Newfoundland.

3.4 TWIN SISTERS ULTRAMAFIC – WASHINGTON

The Twin Sisters massif, located in the northern Cascade Range of Washington State, consists of a relatively unserpentinized body of dunite and harzburgite approximately 17 km long and 7 km wide. It is located along a major thrust fault (Misch 1966) and is in fault contact with Palaeozoic limestone, volcanics and clastic sedimentary rocks. The massif has been interpreted as a slice of continental upper mantle (Christensen 1971a) and as part of an ophiolite complex (Vance *et al.* 1980; Whetten *et al.* 1980).

Petrographic textural observations of the Twin Sisters ultramafic demonstrate its tectonite nature (Ragan 1963). Olivine shows a strong preferred orientation which is relatively consistent over the whole massif. Laboratory measurements of compressional-wave velocities to confining pressures of 10 kbar show strong seismic anisotropy (Christensen 1971a). Composite fabric diagrams obtained from sample locations shown in Fig. 7 are given in Fig. 3. Calculated anisotropies from this composite are illustrated in Fig. 4.

3.5 DUN MOUNTAIN OPHIOLITE BELT – NEW ZEALAND

The Dun Mountain ophiolite belt (Fig. 8), consisting of mafic and ultramafic rocks, is a major geological feature of the South Island of New Zealand, extending for a length of over 1100 km (Coombs *et al.* 1976). It is divided into two segments separated by the Alpine Fault, a northern or Nelson Belt and a southern or Otago Belt. The two segments, considered to have been once continuous, are now separated by 480 km of dextral shift on the Alpine Fault.

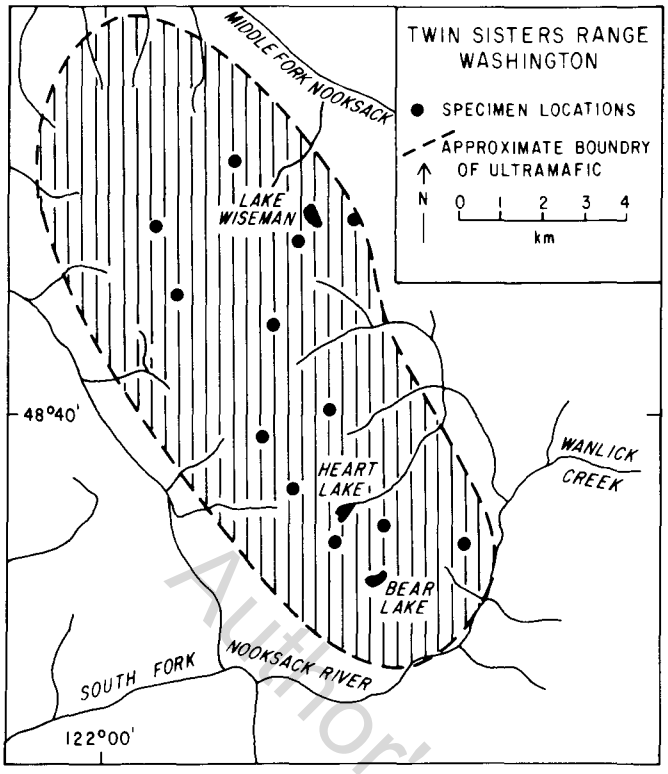

Figure 7. Sample locations from the Twin Sisters ultramafic, Washington, USA.

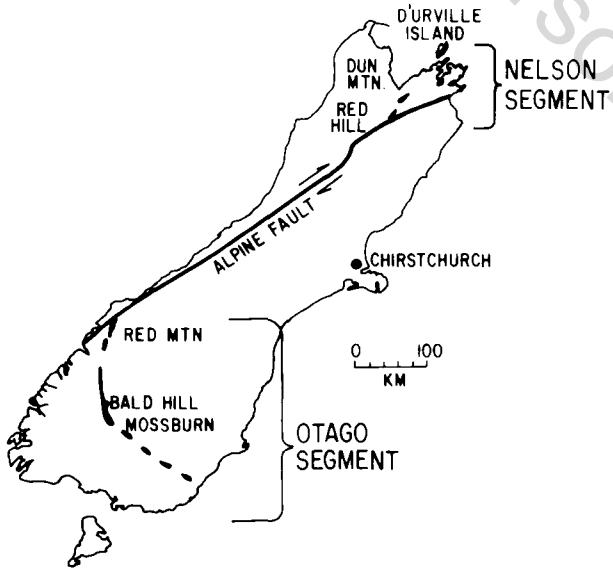

Figure 8. The Dun Mountain ophiolite belt, New Zealand.

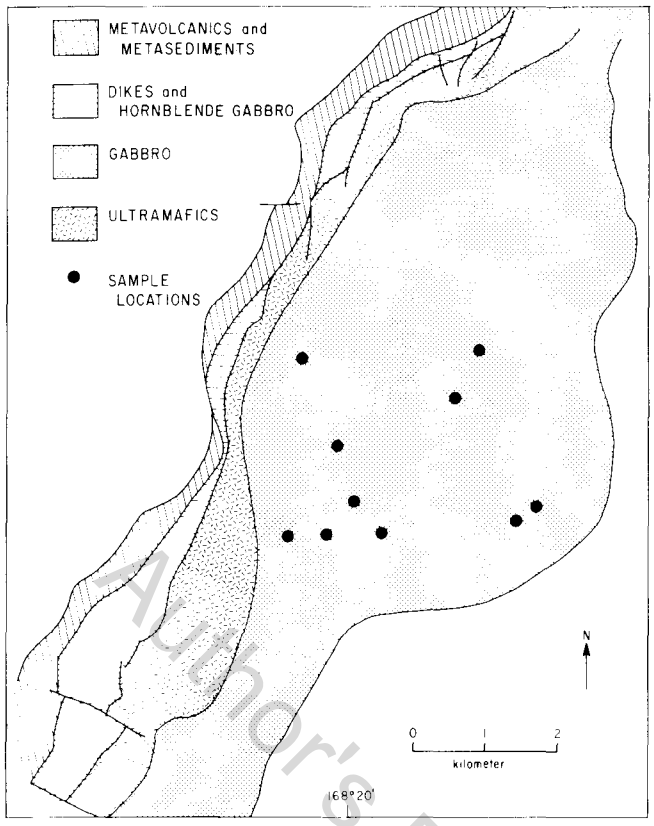

Figure 9. Geology and sample locations from Red Mountain, New Zealand.

Red Mountain (Coombs *et al.* 1976; Sinton 1977) located in the Otago segment is the best preserved ophiolite section of the Dun Mountain belt (Fig. 9). The crustal section contains metavolcanic greenschists with relic pillow structures, a dyke complex of mafic to intermediate composition, plagiogranite, and anorthositic and hornblende-clinopyroxene gabbros often interlayered with ultramafic rocks. The ultramafic sequence, consisting primarily of dunite and harzburgite, is relatively unaltered in the central portion of Red Mountain and partially serpentinized along the margins. Olivine within the ultramafic rocks shows strong preferred orientation (Wilkens 1981) which produces a strong seismic anisotropy. Composite olivine fabrics and calculated seismic anisotropies (Wilkens 1981) are shown in Figs 3 and 4.

Dun Mountain, the type locality for dunite, is located within the Nelson segment of the ophiolite belt and consists of a relatively small (4 km^2) outcrop area of dunite and harzburgite. The ultramafics are unaltered except near the margins where serpentinite is common. Petrographic examination of the ultramafic shows a strong tectonite fabric and field oriented samples (Fig. 10) display a uniform fabric throughout the massif (Fig. 3). Seismic anisotropies calculated from the composite fabric diagrams are shown in Fig. 4.

Red Hills (Walcott 1969) is located approximately 40 km south-west of Dun Mountain. With over 1 km of exposed vertical section and an outcrop area of approximately 110 km^2, the Red Hills massif is the largest and best exposed ultramafic of the Nelson segment. To

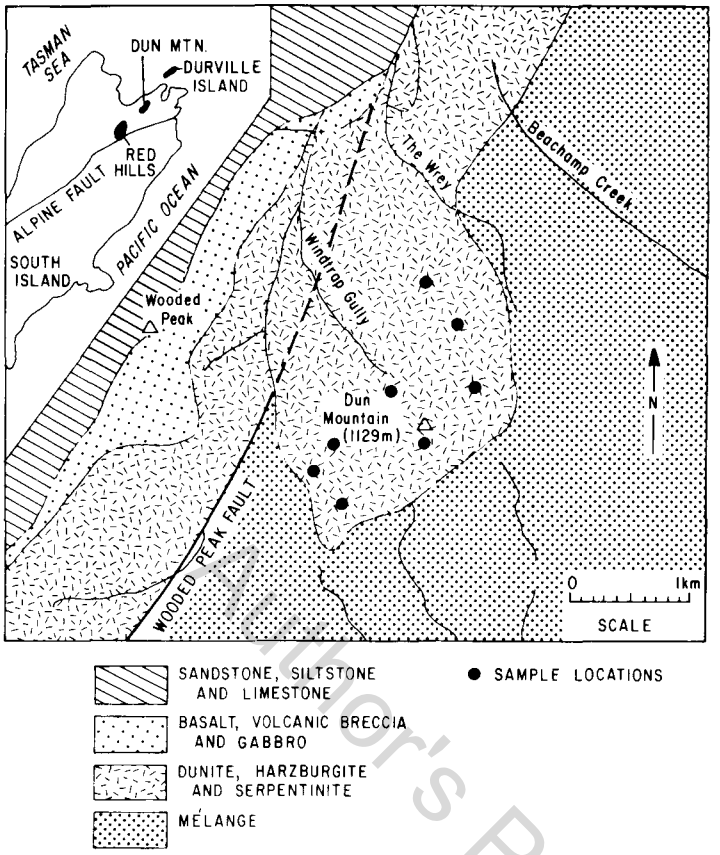

Figure 10. Sample locations from Dun Mountain, New Zealand.

the north and west, crustal rocks consisting of basalt and gabbro dykes and sills occur in fault contact with the ultramafic (Davis *et al.* 1980). At Red Hills numerous faults bound and crosscut the ultramafic and detailed mapping by Walcott (1969) has shown the presence of a major fold in the south central portion of the ultramafic. This folding is also reflected in the olivine fabrics. However, along the western margin of the ultramafics (Fig. 11) olivine fabrics show consistent orientation patterns, producing the olivine composite given in Fig. 3. Calculated anisotropies for this portion of Red Hills are shown in Fig. 4.

4 Accessory minerals

In addition to olivine, a common mineral within ultramafic rocks of probable upper mantle origin is orthopyroxene. Comparisons of single crystal olivine velocities (Verma 1960; Kumazawa & Anderson 1969) with single crystal orthopyroxene velocities (Frisillo & Barsch 1972; Kumuzawa 1969) and dunite velocities (Birch 1960; Christensen 1966; Christensen & Ramananantoandro 1971) with pyroxenite velocities (Birch 1960; Babuška 1972) show that compressional- and shear-wave velocities in pyroxene are generally lower than in olivine of similar composition and hence velocities in peridotites decrease with increasing pyroxene content. In addition, the amount of pyroxene in an ultramafic rock will have a significant effect on anisotropy.

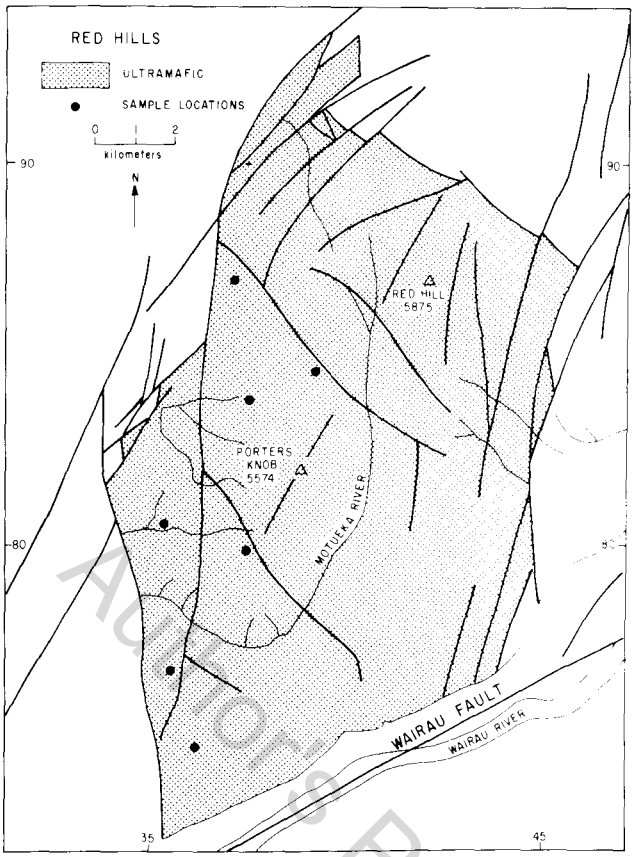

Figure 11. Sample locations from Red Hills, New Zealand.

If accessory orthopyroxene in peridotite has a random orientation its presence will dilute the anisotropy produced by preferred olivine orientation and seismic anisotropy will decrease with increasing pyroxene content. Since single crystal orthopyroxene like olivine is highly anisotropic (Fig. 12) a preferred orientation of orthopyroxene will modify the anisotropy produced by preferred olivine orientation. The resultant anisotropy will depend upon the percentage of pyroxene in the upper mantle, the degree of preferred orientation of olivine and orthopyroxene and the spatial relationship of the olivine axis concentrations to the orthopyroxene axis concentrations. If the olivine *a*-, *b*- and *c*-axes parallel to the orthopyroxene *a*-, *b*- and *c*-axes, respectively, the contribution of orthopyroxene to total anisotropy will reinforce the anisotropy produced by the olivine (Fig. 12) and since pyroxene is less anisotropic than olivine increasing the pyroxene content will only slightly reduce the rock anisotropy. On the other hand, if the maximum concentrations of olivine *a*- and *b*-axes parallel the orthopyroxene *b*- and *a*-axes, respectively, the presence of pyroxene will significantly lower the resultant anisotropy (Fig. 12). Thus a rock with strong preferred olivine orientation could have low compressional-wave anisotropy if the anisotropy produced by the olivine is reduced by orthopyroxene with an appropriate orientation.

A study of mineral orientations in ultramafics from the Bay of Islands ophiolite, Newfoundland (Christensen & Lundquist 1982), suggests that within the upper mantle neither of the above relationships between olivine and pyroxene orientations exist. Instead,

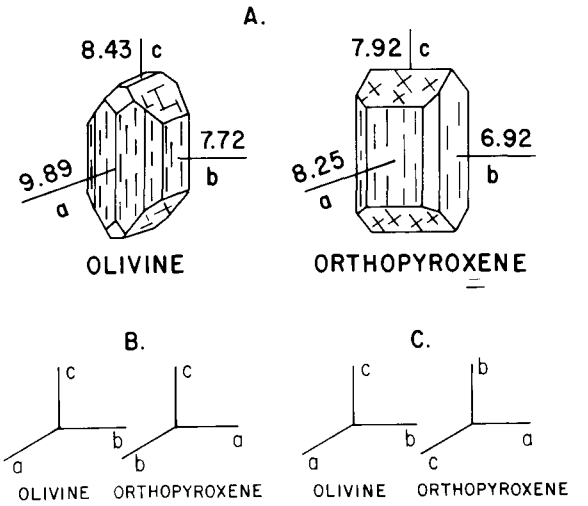

Figure 12. Compressional wave velocities in km s^{-1} along the crystallographic axes of olivine and orthopyroxene. Three possibilities are illustrated for the orientation of olivine relative to orthopyroxene in the upper mantle (see text).

the orthopyroxene *c* crystallographic maxima coincide with the olivine *a*-axes maxima and the orthophyroxene *a*-axes maxima parallel the olivine *b*-axes maxima (Fig. 12). The orientations of the gabbro ultramafic contact and the sheeted dykes within the ophiolite relative to the mineral axes orientations indicate that the olivine *a*- and orthopyroxene *c*-axes are lined within the oceanic upper mantle subparallel to the spreading direction, whereas the olivine *b*-axes maxima and orthopyroxene *a*-axes maxima are approximately perpendicular to the Mohorovičić discontinuity (i.e. vertical). This relationship between olivine and pyroxene fabrics observed in the Bay of Islands ultramafic appears to be common in many ophiolites (e.g. Nicolas *et al.* 1971; Christensen & Lundquist 1982) and thus is likely to be present in the upper oceanic mantle.

The influence of pyroxene content on anisotropy for a section of peridotite from the Bay of Islands ophiolite is shown in Fig. 13. The velocities were calculated from petrofabric analyses of ultramafic rocks over an outcrop area of 80 km^2. The velocities in Fig. 13 are for pressures of 2 kbar and room temperature. Note that increasing pyroxene content lowers compressional-wave velocities, decreases compressional-wave anisotropy, and decreases the difference in shear velocities associated with shear-wave splitting. However, the symmetry of the anisotropy remains essentially intact.

The velocities presented in Figs 3 and 13 have been calculated at approximately 25°C. Within the upper few kilometres of the mantle it is estimated that temperatures generally are between 200 and 500°C (e.g. Blackwell 1971). Laboratory measurements of the effect of temperature on velocities (e.g. Birch 1943; Kern 1978; Ramananantoandro & Manghnani 1978; Christensen 1979) demonstrate that an increase in temperature of 100°C will generally lower velocities by less than 1 per cent. These measurements also show that temperature has little effect on anisotropy. Thus to extrapolate to *in situ* conditions the compressional wave velocities on Figs 4 and 13 should be lowered a few per cent; however, the shear-wave splitting and compressional-wave anisotropy are not apparently temperature dependent.

Mantle anisotropy observed from seismic refraction studies is usually two-dimensional

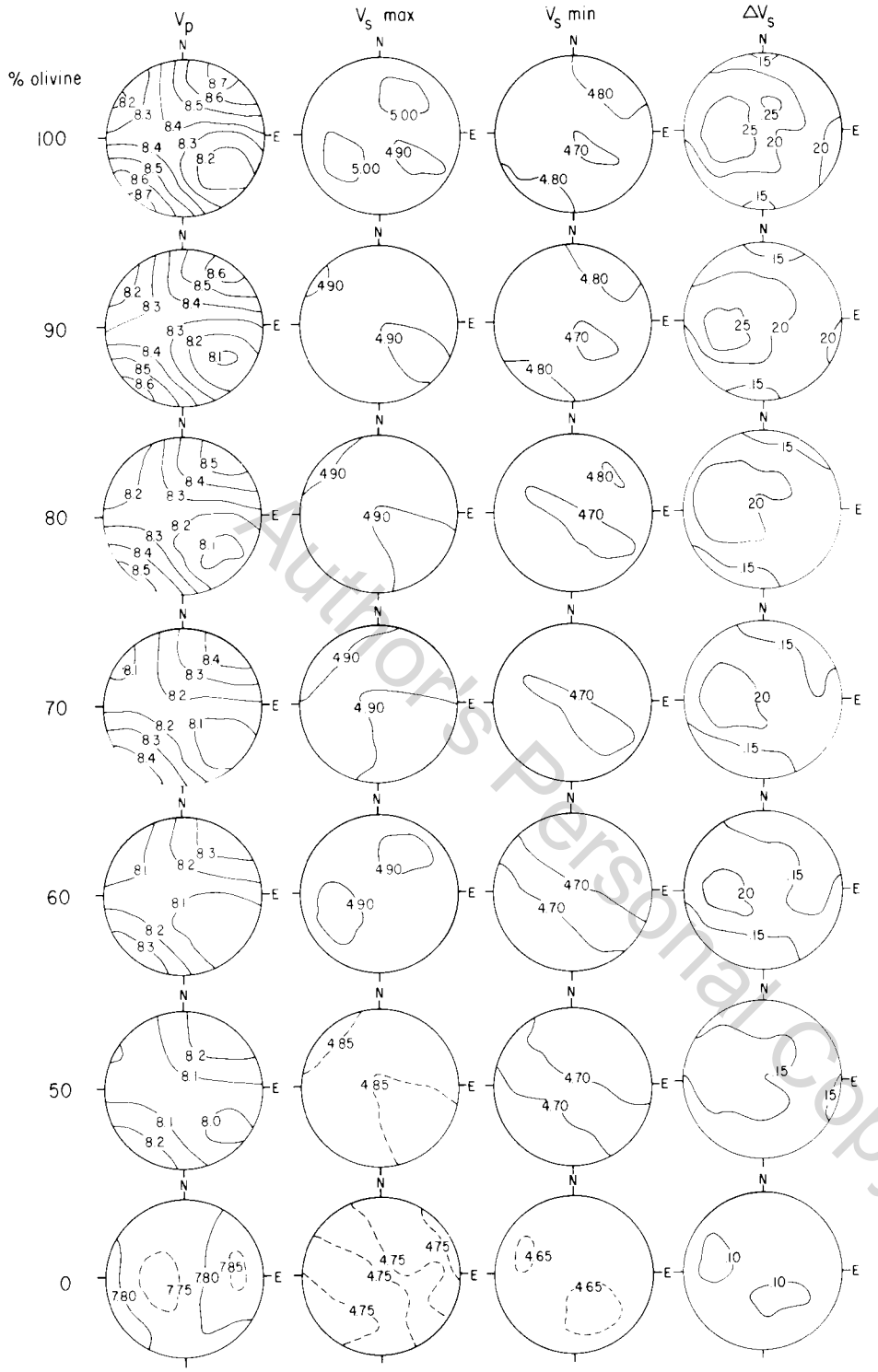

Figure 13. Variations in direction of compressional wave velocity (V_P) and shear-wave splitting (ΔV_S) in km s^{-1} for varying proportions of olivine and orthopyroxene. Data from North Arm Mountain, Bay of Islands, Newfoundland (Christensen & Lundquist 1982).

Table 1. Least-squares solutions to the Backus equation for varying pyroxene contents (Christensen & Lundquist 1982).

Pyroxene (per cent)	V_0	B	C	E	F
0	8.54	−0.52	−2.86	0.15	0.08
10	8.47	−0.65	−2.52	0.13	0.10
20	8.39	−0.50	−2.25	0.08	0.06
30	8.31	−0.58	−2.08	0.02	0.01
40	8.24	−0.37	−1.92	0.10	−0.03
50	8.16	−0.48	−1.65	0.03	−0.04

and within a horizontal plane immediately below the Mohorovičić discontinuity. The equation relating compressional-wave velocity (V_P) to azimuth (ϕ) is given by

$$V_P^2 = V_0^2 + B\cos 2\phi + C\sin 2\phi + E\cos 4\phi + F\sin 4\phi$$

where V_0 is mean velocity and B, C, E and F are constants (Backus 1965). Least squares solutions from the Bay of Islands ophiolite within a plane parallel to the gabbro ultramafic contact (Table 1) clearly show the decrease in mean velocity and anisotropy associated with increasing pyroxene content. Furthermore, the 4ϕ terms of the Backus equation appear to be statistically insignificant (Christensen & Lundquist 1982).

In addition to orthopyroxene and olivine, other minerals which are likely constituents of the uppermost mantle and would thus be important in anisotropy considerations include clinopyroxene, plagioclase, hornblende and spinel (e.g. Ringwood 1974). Measurements of velocities in single crystals of plagioclase, hornblende and clinopyroxene show high anisotropy; however, these minerals are not particularly abundant in the ultramafic sections of many ophiolites and are thus unlikely to contribute significantly to upper mantle anisotropy. Spinel is a common accessory mineral in many ultramafic rocks; however, it is relatively low in anisotropy as is garnet (Carter *et al.* 1972).

5 Conclusions

Large slabs of ultramafic mantle which have been tectonically emplaced along faults provide valuable information on the nature of upper mantle seismic anisotropy. Based on fabric analyses it can be demonstrated that within the ultramafic massifs olivine possesses a consistent orientation over large areas. The common fabric consists of a strong olivine *a* crystallographic maxima and partial girdles of olivine *b*- and *c*-axes (Fig. 3). In ultramafic rocks which are clearly part of an ophiolite sequence, the olivine *a*-axes are usually oriented subparallel to the spreading direction, which is inferred by the orientations of sheeted dykes (Christensen & Salisbury 1979; Christensen & Smewing 1981). This relationship is illustrated schematically in Fig. 14. Since olivine is fast for compressional-wave propagation parallel to its *a*-axis, seismic anisotropies measured by marine refraction studies show fast compressional-wave velocities subparallel to spreading directions.

Shear-wave splitting is common in ultramafic rocks and also originates primarily from preferred olivine orientation. The fabric analyses and calculated shear anisotropies presented in Fig. 4 show that the maximum shear-wave splitting does not coincide with the direction of maximum velocity. As has been emphasized by Crampin (1981), shear-wave splitting observations are particularly valuable for detecting the presence of anisotropy, especially in regions which contain both anisotropic and isotropic rock (Fig. 15). Observations of the magnitude of shear-wave splitting and comparisons of azimuthal variations of shear-wave splitting with compressional-wave anisotropy will in the future provide much information

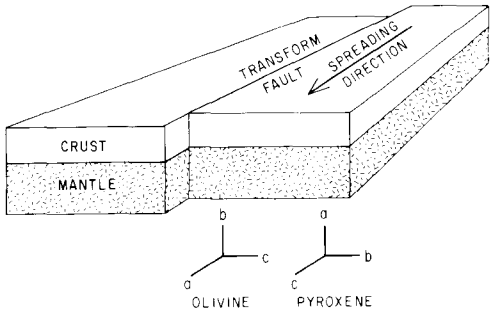

Figure 14. The ideal orientations of olivine and orthopyroxene in the oceanic upper mantle.

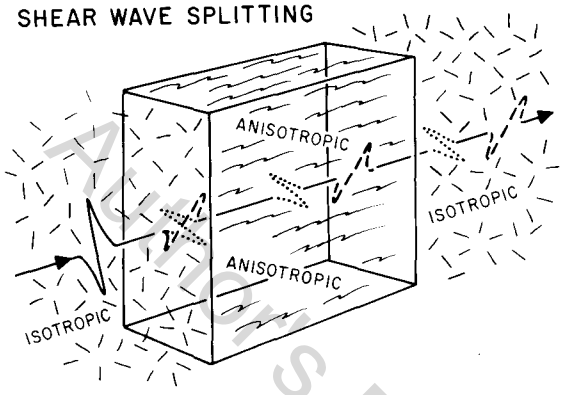

Figure 15. Shear-wave splitting in anisotropic rock (Crampin 1981).

on the nature of preferred mineral orientation in the Earth's mantle as well as its composition.

In addition to preferred olivine orientation, seismic anisotropy within the upper mantle is related to accessory minerals, the most important being orthopyroxene. It is likely that within some regions of the upper mantle orthopyroxene constitutes over 30 per cent by volume of the upper mantle (Christensen & Lundquist 1982). Orthopyroxene often has a strong fabric, with crystallographic *a*-, *b*- and *c*-axes concentrations parallel to olivine *b*, *c* and *a* concentrations, respectively. The fastest direction in orthopyroxene (crystallographic *a*) is likely to be nearly vertical in the upper mantle. Within the plane of the Mohorovičić discontinuity (that is, for P_n propagation) the maximum velocity produced from preferred olivine orientation will parallel the maximum velocity produced by orthopyroxene orientation and thus anisotropy decreases only slightly with increasing pyroxene content.

Considering their varying ages and wide range in geographic distribution, it is remarkable that the anisotropies of the ultramafic massifs show such similarities in magnitude and symmetry (Fig. 4). This suggests that seismic anisotropy has been a property of the upper mantle throughout much of geological time and is world-wide in occurrence. The latter is supported by current seismic refraction data (Fig. 1) although only a two-dimensional picture of compressional-wave anisotropy is provided by such investigations. The data presented here are useful in that the complete three-dimensional anisotropy is obtained, which includes shear-wave velocities as well as compressional-wave velocities. With new

seismic anisotropy field experiments designed specifically to investigated three-dimensional upper mantle anisotropy, a more detailed comparison will hopefully be possible in the future.

Acknowledgments

This research was supported by the Office of Naval Research Contract No. N-00014-80-C-0252. The help of J. Smewing, R. Wilkens and M. Salisbury in collecting samples, and L. Slater, S. Lundquist, R. Prior and R. Wilkens in petrofabric analysis is greatly appreciated.

References

Babuška, V., 1972. Elasticity and anisotropy of dunite and bronzitite, *J. geophys. Res.*, **77**, 6955–6965.

Backus, G. E., 1965. Possible forms of seismic anisotropy of the uppermost mantle under oceans, *J. geophys. Res.*, **70**, 3429–3439.

Baker, D. W. & Carter, N. L., 1972. Seismic velocity anisotropy calculated for ultramafic minerals and aggregates, in *Flow and Fracture of Rocks*, eds Heard, I. Y., Carter, N. L. & Raleigh, C. B., *Monogr. Am. geophys. Un.*, **16**, 157–166.

Bamford, D., 1977. P_n velocity anisotropy in a continental upper mantle, *Geophys. J. R. astr. Soc.*, **49**, 29–48.

Bamford, D., Jentsch, M. & Prodehl, C., 1979. P_n anisotropy studies in northern Britain and the eastern and western United States, *Geophys. J. R. astr. Soc.*, **57**, 397–430.

Birch, F., 1943. Elasticity of igneous rocks at high temperatures and pressures, *Bull. geol. Soc. Am.*, **54**, 263–286.

Birch, F., 1960. The velocity of compressional waves in rocks to 10 kilobars, 1, *J. geophys. Res.*, **65**, 1083–1102.

Birch, F., 1961. The velocity of compressional waves in rocks to 10 kilobars, 2, *J. geophys. Res.*, **66**, 2199–2224.

Blackwell, D. D., 1971. The thermal structure of the continental crust, in *The Structure and Physical Properties of the Earth's Crust*, ed. Heacock, J. *Monogr. Am. geophys. Un.*, **14**, 169–184.

Carter, N. L., Baker, D. W. & George, R. P. (Jr), 1972. Seismic anisotropy, flow, and constitution of the upper mantle, in *Flow and Fracture of Rocks*, eds Heard, I. Y., Carter, N. L. & Raleigh, C. B., *Monogr. Am. geophys. Un.*, **16**, 167–190.

Christensen, N. I., 1966. Elasticity of ultrabasic rocks, *J. geophys. Res.*, **71**, 5921–5931.

Christensen, N. I., 1971a. Fabric, seismic anisotropy, and tectonic history of the Twin Sisters dunite, Washington, *Bull. geol. Soc. Am.*, **82**, 1681–1694.

Christensen, N. I., 1971b. Shear wave propagation in rocks, *Nature*, **229**, 549–550.

Christensen, N. I., 1979. Compressional wave velocities in rocks and high temperatures and pressures, critical thermal gradients, and crustal low-velocity zones, *J. geophys. Res.*, **84**, 6849–6857.

Christensen, N. I. & Lundquist, S. M., 1982. Pyroxene orientation within the upper mantle, *Bull. geol. Soc. Am.*, **93**, 279–288.

Christensen, N. I. & Ramananantoandro, R., 1971. Elastic moduli and anisotropy of dunite to 10 kilobars, *J. geophys. Res.*, **76**, 4003–4010.

Christensen, N. I. & Salisbury, M. H., 1979. Seismic anisotropy in the oceanic upper mantle: evidence from the Bay of Islands ophiolite complex, *J. geophys. Res.*, **84**, 4601–4610.

Christensen, N. I. & Smewing, J. D., 1981. Geology and seismic structure of the northern section of the Oman ophiolite, *J. geophys. Res.*, **86**, 2545–2555.

Church, W. R., 1972. Ophiolite: its definition, origin as ocean crust, and mode of emplacement in orogenic belts, with special reference to the Appalachians, *Publs Dept Energy, Mines Res, Can.*, **42**, 71–85.

Coleman, R. G., 1981. Tectonic setting for ophiolite obduction in Oman, *J. geophys. Res.*, **86**, 2497–2503.

Coleman, R. G. & Hopson, C. A., 1981. Introduction to the Oman ophiolite Special Issue, *J. geophys. Res.*, **86**, 2495–2496.

Coombs, D. S., Landis, C. A., Norris, R. J., Sinton, J. M., Borns, D. J. & Craw, D., 1976. The Dun Mountain ophiolite belt, New Zealand, its tectonic setting, constitution, and origin, with special reference to the southern portion, *Am. J. Sci.*, **276**, 561–603.

Crampin, S., 1981. A review of wave motion in anisotropic and cracked elastic-media, *Wave Motion,* **3,** 343–391.

Crosson, R. S., Lin, J. W., 1971. Voight and Reuss prediction of anisotropic elasticity of dunite, *J. geophys. Res.,* **76,** 570–578.

Davis, T. E., Johnston, M. R., Rankin, P. C. & Stull, R. J., 1980. The Dun Mountain ophiolite belt in East Nelson, New Zealand, in *Ophiolites Proc. int. Ophiolite Symposium,* Cyprus, 1979, pp. 480–496, ed. Panayiotou, A., Ministry of Agriculture and Natural Resources Geological Survey Department, Republic of Cyprus.

Dziewonski, A. M. & Anderson, D. L., 1981. Preliminary reference Earth model, *Phys. Earth planet. Int.,* **25,** 297–356.

Francis, T. J. G., 1969. Generation of seismic anisotropy in the upper mantle along the mid-oceanic ridges, *Nature,* **221,** 162–165.

Frisillo, A. L. & Barsch, G. R., 1972. Measurement of single-crystal elastic constants of bronzite as a function of pressure and temperature, *J. geophys. Res.,* **77,** 6360–6383.

Fuchs, K., 1983. Recently formed elastic anisotropy and petrological models for the continental subcrustal lithosphere in southern Germany, *Phys. Earth planet. Int.,* **31,** 93–118.

Gass, I. G. & Smewing, J. D., 1973. Intrusion, extrusion and metamorphism at constructive margins: evidence from the Troodos massif, Cyprus, *Nature,* **242,** 26–29.

George, R. P., 1978. Structural petrology of the Olympus ultramafic complex in the Troodos ophiolite, Cyprus, *Bull. geol. Soc. Am.,* **89,** 845–865.

Girardeau, J. & Nicolas, A., 1981. The structures of two ophiolite massifs, Bay-of-Islands, Newfoundland: a model for the ocean crust and upper mantle, *Tectonophys.,* **77,** 1–34.

Glennie, K. W., Bouef, M. G. A., Hughes-Clarke, M. W., Moody-Stuart, M., Pilaar, W. F. H. & Reinhardt, B. M., 1974. Geology of the Oman Mountains, Part one (text), Part two (tables and illustrations), Part three (enclosures), *Verh. K. ned. geol. mijnb. Genoot.,* **31,** 423 pp.

Greenbaum, D., 1972. Magmatic processes at ocean ridges: evidence from the Troodos massif, Cyprus, *Nature,* **238,** 18–21.

Hess, H. H., 1964. Seismic anisotropy of the uppermost mantle under oceans, *Nature,* **203,** 629–631.

Hopson, C. A., Coleman, R. G., Gregory, R. T., Pallister, J. S. & Bailey, E. H., 1981. Geological section through the Samail ophiolite and associated rocks along a muscat-ibra transect, south-eastern Oman Mountains, *J. geophys. Res.,* **86,** 2527–2544.

Kamb, W. B., 1959. Ice petrofabric observations from the Blue Glacier, Washington, in relation to theory and experiment, *J. geophys. Res.,* **64,** 1891–1909.

Karson, J. A., 1982. Reconstructed seismic velocity structure of the Lewis Hills massif and implications for oceanic fracture zones, *J. geophys. Res.,* **87,** 961–978.

Keen, C. E. & Barrett, D. L., 1971. A measurement of seismic anisotropy in the Northeast Pacific, *Can. J. Earth Sci.,* **8,** 1056–1064.

Kern, H., 1978. The effect of high temperature and high confining pressure on compressional wave velocities in quartz-bearing and quartz-free igneous and metamorphic rocks, *Tectonophys.,* **44,** 185–203.

Klima, K. & Babuška, V., 1968. A comparison of measured and calculated elastic anisotropies of marble, *Studie geophys. geod.,* **12,** 377–384.

Kumazawa, M., 1964. The elastic constants of rock in terms of elastic constants of constituent mineral grains, petrofabric and interface structures, *J. Earth Sci.,* **72,** 147–176.

Kumazawa, M., 1969. The elastic constants of single-crystal orthopyroxene, *J. geophys. Res.,* **74,** 5973–5980.

Kumazawa, M. & Anderson, O. L., 1969. Elastic moduli, pressure derivatives and temperature derivatives of single crystal olivine and single crystal forsterite, *J. geophys. Res.,* **74,** 5961–5972.

Leven, J., Jackson, I. & Ringwood, A. E., 1981. Upper mantle seismic anisotropy and lithospheric decoupling, *Nature,* **289,** 234–239.

Malecek, S. J. & Clowes, R. M., 1978. Crustal structure near Explorer Ridge from a Marine Deep Seismic Sounding Survey, *J. geophys. Res.,* **83,** 5899–5912.

Misch, P., 1966. Tectonic evolution of the northern Cascades of Washington State, in *Tectonic History and Mineral Deposits of the Western Cordillera, Symp. Can. Inst. min. Metall.,* Montreal, **8,** 101–148.

Moores, E. M. & Vine, F. J., 1971. The Troodos massif, Cyprus, and other ophiolites as oceanic crust: evaluation and implications, *Phil. Trans. R. Soc. A,* **268,** 443–466.

Morris, G. B., Raitt, R. W. & Shor, G. G. (Jr), 1969. Velocity anisotropy and delay-time maps of the mantle near Hawaii, *J. geophys. Res.,* **74,** 4300–4316.

Musgrave, M. J. P., 1970. *Crystal Acoustics,* Holden-Day, San Francisco, 288 pp.

Nicolas, A., Bouchez, J. L., Boudier, F. & Mercier, J. C., 1971. Textures, structures and fabrics due to solid state flow in some European lherzolites, *Tectonophys.,* **12,** 55–86.

Peselnick, L. & Nicolas, A., 1978. Seismic anisotropy in an ophiolite peridotite: application to oceanic upper mantle, *J. geophys. Res.,* **83,** 1227–1235.

Ragan, D. R., 1963. Emplacement of the Twin Sisters Dunite, Washington, *Am. J. Sci.,* **251,** 549–565.

Raitt, R. W., 1963. Seismic refraction studies of the Mendicino fracture zone, *Rep. MPL-U-23/63, Mar. Phys. Lab.,* Scripps Institute of Oceanography, University of California, San Diego.

Raitt, R. W., Shor, G. G. (Jr), Francis, T. J. G. & Morris, G. B., 1969. Anisotropy of the Pacific upper mantle, *J. geophys. Res.,* **74,** 3095–3109.

Raitt, R. W., Shor, G. G. (Jr), Morris, G. B. & Kirk, H. K., 1971. Mantle anisotropy in the Pacific Ocean, *Tectonophys.,* **12,** 173–186.

Raleigh, C. B., 1968. Mechanism of plastic deformation of olivine, *J. geophys. Res.,* **73,** 5391–5406.

Ramananantoandro, R. & Manghnani, M. H., 1978. Temperature dependence of the compressional wave velocity in anisotropic dunite: measurements to 500°C at 10 kbar, *Tectonophys.,* **47,** 73–84.

Ringwood, A. E., 1974. *Composition and Petrology of the Earth's Mantle,* McGraw-Hill, New York, 618 pp.

Shor, G. G. (Jr) & Pollard, D. D., 1964. Mohole site selection studies north of Maui, *J. geophys. Res.,* **69,** 1627–1637.

Shor, G. G. (Jr), Raitt, R. W., Henry, M., Bentley, L. R. & Sutton, G. H., 1973. Anisotropy and crustal structure of the Cocos Plate, *Geofis int.,* **13,** 337–362.

Sinton, J. M., 1977. Equilibration history of the basal alpine-type peridotite, Red Mountain, New Zealand, *J. Petrol.,* **18,** 216–246.

Smewing, J. D., 1981. Mixing characteristics and compositional differences in mantle-derived melts beneath spreading axes: evidence from cyclically layered rocks in the ophiolite of North Oman, *J. geophys. Res.,* **86,** 2645–2659.

Smith, C. H., 1958. Bay of Islands igneous complex Western Newfoundland, *Mem. geol. Surv. Can.,* **290,** 2534, 132 pp.

Snydsman, W. E., Lewis, B. T. R. & McClain, J., 1975. Upper mantle velocities on the northern Cocos Plate, *Earth planet. Sci. Lett.,* **28,** 46–50.

Vance, J. A., Dungan, M. A., Blanchard, C. P. & Rhodes, J. M., 1980. Tectonic setting and trace element geochemistry of Mesozoic ophiolitic rocks in Western Washington, *Am. J. Sci.,* **280-A,** 359–388.

Verma, R. K., 1960. Elasticity of some high-density crystals, *J. geophys. Res.,* **65,** 757–766.

Vetter, E. & Minster, J., 1981. P_n velocity anisotropy in southern California, *Bull. seism. Soc. Am.,* **71,** 1511–1530.

Walcott, R. I., 1969. Geology of the Red Hills Complex, Nelson, New Zealand, *Trans. R. Soc. N. Z.,* **7,** 57–88.

Whetten, J. T., Zartman, R. E., Blakely, R. J. & Jones, D. L., 1980. Allochthonous Jurassic ophiolite in Northwest Washington, *Bull. geol. Soc. Am.,* **81,** 359–368.

Wilkens, R. H., 1981. Seismic properties and petrofabrics of ultramafic and mafic rocks from the Red Mountain ophiolite, New Zealand, *PhD thesis,* University of Washington, 159 pp.

Williams, H., 1973. The Bay of Islands map area, Newfoundland, *Pap. geol. Surv. Can.,* **72-34,** 1–7.

Williams, H. & Malpas, J., 1972. Sheeted dikes and brecciated dike rocks within transported igneous complexes, Bay of Islands, Western Newfoundland, *Can. J. Earth Sci.,* **9,** 1216–1229.

Williams, H. & Stevens, R. K., 1974. The ancient continental margin of eastern North America, in *The Geology of Continental Margins,* pp. 781–796, eds Burk, C. A. & Drake, C. L., Springer-Verlag, Berlin.

Wilson, R. A. M., 1959. The geology of the Xeros-Troodos area, *Mem. geol. Surv. Dep. Cyprus,* **1,** 1–135.